AD-A054 947 SYRACUSE UNIV NY DEPT OF MECHANICAL AND AEROSPACE E--ETC F/G 13/4
IMPACT STRESSES IN FLAT-PACK LIDS AND BASES.(U)
APR 78 C LIBOVE F30602-75-C-0121
UNCLASSIFIED MAE-1229-T-1 RADC-TR-78-98 NL

1 OF 1
AD A054947

END
DATE FILMED
7-78
DDC

RADC-TR-78-98
Final Technical Report
April 1978

IMPACT STRESSES IN FLAT-PACK LIDS AND BASES

Charles Libove

Syracuse University

Approved for public release; distribution unlimited.

ROME AIR DEVELOPMENT CENTER
Air Force Systems Command
Griffiss Air Force Base, New York 13441

This report has been reviewed by the RADC Information Office (OI) and is releasable to the National Technical Information Service (NTIS). At NTIS it will be releasable to the general public, including foreign nations.

RADC-TR-78-98 has been reviewed and is approved for publication.

APPROVED: Peter F. Manno

PETER F. MANNO
Project Engineer

APPROVED: Joseph J. Naresky

JOSEPH J. NARESKY
Chief, Reliability & Compatibility Division

FOR THE COMMANDER: John P. Huss

JOHN P. HUSS
Acting Chief, Plans Office

If your address has changed or if you wish to be removed from the RADC mailing list, or if the addressee is no longer employed by your organization, please notify RADC (RBRM) Griffiss AFB NY 13441. This will assist us in maintaining a current mailing list.

Do not return this copy. Retain or destroy.

MISSION
of
Rome Air Development Center

RADC plans and conducts research, exploratory and advanced development programs in command, control, and communications (C^3) activities, and in the C^3 areas of information sciences and intelligence. The principal technical mission areas are communications, electromagnetic guidance and control, surveillance of ground and aerospace objects, intelligence data collection and handling, information system technology, ionospheric propagation, solid state sciences, microwave physics and electronic reliability, maintainability and compatibility.

UNCLASSIFIED

(14) MAE-1229-T-1

SECURITY CLASSIFICATION OF THIS PAGE *(When Data Entered)*

(19) **REPORT DOCUMENTATION PAGE**

READ INSTRUCTIONS BEFORE COMPLETING FORM

(18) 1. REPORT NUMBER: RADC-TR-78-98

2. GOVT ACCESSION NO.

3. RECIPIENT'S CATALOG NUMBER

(6) 4. TITLE *(and Subtitle)*: IMPACT STRESSES IN FLAT-PACK LIDS AND BASES

(9) 5. TYPE OF REPORT & PERIOD COVERED: Final Technical Report

6. PERFORMING ORG. REPORT NUMBER: MAE-1229-T1

(10) 7. AUTHOR(s): Charles Libove

(15) 8. CONTRACT OR GRANT NUMBER(s): F30602-75-C-0121

9. PERFORMING ORGANIZATION NAME AND ADDRESS
Syracuse University
139 E. A. Link Hall
Syracuse NY 13210

(16) (17) 10. PROGRAM ELEMENT, PROJECT, TASK AREA & WORK UNIT NUMBERS: 61102F 2306J4P2 J4

(11) 11. CONTROLLING OFFICE NAME AND ADDRESS
Rome Air Development Center (RBRM)
Griffiss AFB NY 13441

12. REPORT DATE: Apr 1978

13. NUMBER OF PAGES: 40

(12) 45p.

14. MONITORING AGENCY NAME & ADDRESS *(if different from Controlling Office)*: Same

15. SECURITY CLASS. *(of this report)*: UNCLASSIFIED

15a. DECLASSIFICATION/DOWNGRADING SCHEDULE: N/A

16. DISTRIBUTION STATEMENT *(of this Report)*

Approved for public release; distribution unlimited.

DDC RECEIVED JUN 13 1978 F

17. DISTRIBUTION STATEMENT *(of the abstract entered in Block 20, if different from Report)*

Same

18. SUPPLEMENTARY NOTES

RADC Project Engineer: Peter F. Manno (RBRM)

19. KEY WORDS *(Continue on reverse side if necessary and identify by block number)*

flat-pack	dynamic	flatwise impact	inelastic
stress	drop test	lids	hydrostatic pressure
strain	mechanical screen	bases	
static	edgewise impact	elastic	

20. ABSTRACT *(Continue on reverse side if necessary and identify by block number)*

An analysis is made of the "normal handling" that a microelectronic package is likely to encounter. The stresses and deformations of the lids and bases of a rectangular flat-pack caused by the accidental dropping of the package onto a floor from a height of a few feet, are assessed theoretically. The results of the study shows that the assumed normal handling conditions constitutes a severe environment which is capable of producing stress that will buckle a metallic lid or crack a ceramic lid or base.

DD FORM 1 JAN 73 1473 EDITION OF 1 NOV 65 IS OBSOLETE

UNCLASSIFIED

SECURITY CLASSIFICATION OF THIS PAGE *(When Data Entered)*

400 224

CONTENTS

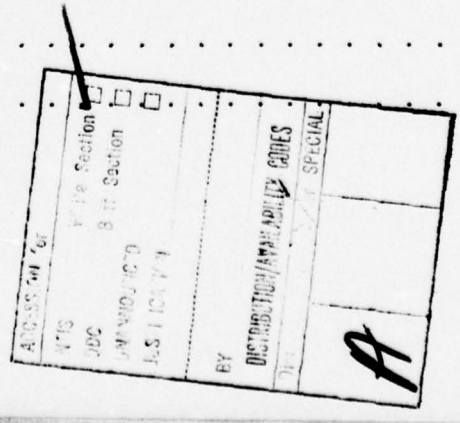

EVALUATION

The objective of this effort was to provide a means for theoretically predicting the stresses and deflections produced in rectangular flat-pack lids and bases by normal handling procedures. For this study, normal handling was considered to be the accidental dropping of a package onto a floor from a height of several feet.

Mathematical models were developed to theoretically predict the stresses and deformations in the lids and bases of rectangular flat-packs caused by the resulting impact of the package onto the floor. The study took into account the package landing on either the edgewise or flatwise axis. Significant results are as follows:

a. The stresses induced by such normal handling can be severe enough to buckle a metallic lid or crack a ceramic lid or base.

b. A screening procedure appears to be feasible whereby packages most vulnerable to handling damage can be identified.

c. A dynamic test consisting of a hammer striking an initially stationary package is presented to simulate the actual dropping of the package.

d. Static tests consisting of mounting the package in a universal testing machine for the edgewise impact and subjecting the package to external hydrostatic pressure in a pressure vessel to simulate the flatwise impact are presented.

The results of this study will be verified experimentally and will be extended to include the effects of the impact on the internal components of the package, such as wires, wire bonds, dies and substrates.

The overall results of this effort will be used by RADC in the development of screening procedures for MIL-STD-883, "Test Methods and Procedures for Microelectronics" and in support of the Air Force/NASA task to establish screening requirements for Class S hybrids.

Peter F. Manno

PETER F. MANNO
Project Engineer

I. INTRODUCTION

It has been said that "normal handling" is one of the severest environments that a microelectronic package is likely to encounter. In this report we interpret normal handling to be the accidental dropping of the package onto a floor from a height of a few feet, and we assess theoretically the stresses and deformations caused by the resulting impact, with particular reference to the lid and base of a rectangular flat-pack.

For the purpose of this study we consider two idealized modes of impact: edgewise and flatwise, as illustrated in Figure 1. In the main our study will apply to the constant-thickness single-material lid or base shown in cross section in Figure 2(a). However, where it is not too difficult to do so, we shall extend our analysis to lids whose edges are thinned down to a small fraction of the thickness of the main part (Figure 2(b)) and to bases made of two components bonded together over their entire contact plane (Figure 2(c)).

The study will show that the kind of normal handling we have assumed is indeed a severe environment, capable of producing stresses that will buckle a metallic lid or crack a ceramic lid or base. Static and dynamic tests are suggested that can simulate this environment for screening purposes, and experiments are proposed for testing the accuracy and validity of the theoretical results.

Acknowledgement.- This work was performed under Contract No. F30602-75-C-0121 with the Rome Air Development Center and was suggested by Peter Manno, John Farrell and Edward O'Connell of that Center. Their suggestion of the study and their helpful discussions with the author are gratefully acknowledged.

II. EDGEWISE IMPACT

A. Elastic.- The single-component lid or base impacting edgewise with velocity v on a rigid surface (Figure 3) can, in first approximation, be treated as a uniform rod. When the material is linearly elastic (obeys Hooke's law), the classical theory of impact for a rod (Reference 1) indicates that a compressive stress σ will start to propagate upward immediately upon contact, travel with the speed of sound c in the material, and eventually encompass the entire length of the lid or base (Figures 3(c) and (d)). A tensile stress of the same magnitude will then propagate downward, cancelling out the compressive stress as it goes (Figure 3(e)).

If E is the Young's modulus of the material and ρ its density, the magnitude of the compressive stress will be

$$\sigma = \frac{v}{c} E \tag{1}$$

where

$$c = \sqrt{E/\rho} \tag{2}$$

is the speed of sound in the material. Supposing that the velocity v is due to a free fall from a height h, we may write

$$v = \sqrt{2gh} \tag{3}$$

where g = acceleration of gravity = 32.2 ft/sec^2 = 386 in/sec^2 = 9.8 m/s^2. Using this to eliminate v in Eq. (1), and Eq. (2) to eliminate c, we arrive at the following alternate formula for σ:

$$\sigma = \sqrt{2gh\rho E} \tag{4}$$

The compressive strain ε corresponding to σ is σ/E. Thus,

$$\varepsilon = v/c = v\sqrt{\rho/E} = \sqrt{2gh\rho/E} \tag{5}$$

In a free fall from a small height, v and h are rather small, but E is generally very large; therefore Eq. (1) or (4) can lead to significant stresses. For example, let us consider two specific materials, a Kovar lid and a ceramic base with the following properties:

	Kovar	Ceramic
E $(lb/in.^2)$	20×10^6	47×10^6
E (lb/ft^2)	2880×10^6	6800×10^6
ρ $(lb\text{-}sec^2/ft^4)$	16.2	7.18
$c = \sqrt{E/\rho}$ (ft/sec)	13,300	30,700

An impact velocity of 16 ft/sec, which corresponds to a 4-foot drop, will lead to a compressive stress of

$$\sigma = \frac{v}{c} E = \frac{16}{13,300} (20 \times 10^6) = 24,000 \text{ psi} \tag{6}$$

in the Kovar and

$$\sigma = \frac{16}{30,700} (47 \times 10^6) = 24,500 \text{ psi} \tag{7}$$

in the ceramic.

The likelihood of these stresses causing damage can be judged by comparing σ with the compressive buckling stress σ_{cr} of the component under consideration and, in the case of ceramic, with the compressive

strength σ_c of the material. The elastic compressive buckling stress σ_{cr} of the lid or base shown in Figures 3(a) and (b), taking into account the edge fixity furnished by the package walls, is

$$\sigma_{cr} = kE(t/a)^2 \tag{8}$$

where k is the function of b/a given by the solid curve in Figure 4 (adapted from Reference 2). The compressive strength σ_c of a ceramic is generally an item of information supplied by the manufacturer.

For illustrative purposes, let us apply these damage criteria to the Kovar lid and ceramic base considered previously, assuming the following additional characteristics:

	Kovar	Ceramic
a (in.)	.92	.92
b (in.)	2.22	2.22
b/a	2.5	2.5
t (in.)	.010	.030
σ_c (psi)	-----	375,000

From Figure 4 (solid curve) we find that $k = 6.95$, whence Eq. (8) gives the following buckling stresses:

$$\sigma_{cr} = 6.95\ (20 \times 10^6)\left(\frac{.01}{.92}\right)^2 = 16{,}400 \text{ psi} \quad \text{(Kovar)} \tag{9}$$

$$\sigma_{cr} = 6.95\ (47 \times 10^6)\left(\frac{.03}{.92}\right)^2 = 348{,}000 \text{ psi} \quad \text{(Ceramic)} \tag{10}$$

Comparing (6) and (9), we conclude that the Kovar lid is very likely to buckle under its impact-induced compressive stress of 24,000 psi. On the other hand, the corresponding stress of 24,500 psi in the ceramic base (see

Eq. (7)) is well below both the buckling stress, Eq. (10), and the material compressive strength quoted in the table above.

The buckling of a Kovar lid may be tolerable if the out-of-flatness resulting from any permanent buckles is acceptable. In the case of a Kovar base to which a ceramic substrate is attached with only a few bonds, the impact-induced buckling could conceivably damage the bonds and cause separation of the substrate from the base. On the other hand, if the substrate covered the entire base and were bonded to it over the entire contact plane, the ceramic and Kovar together would constitute a two-component base that might be safe against buckling because of its rather large thickness. (The elastic buckling of a two-component base is discussed in Section V.)

In the above buckling considerations, particularly Eq. (8) and Figure 4, we have assumed the impact to occur along the shorter of the two dimensions, as in Figure 3(a), when the two dimensions a and b are unequal. This assumption is based mainly on the buckle pattern obtained in the random dropping of a Kovar package base in which the ratio b/a was 2.5. The observed buckle pattern was clearly the multi-lobed pattern associated with longitudinal compression, rather than the single-lobe pattern associated with transverse compression (see Figure 19).

The use of a buckling stress formula associated with longitudinal compression is further justified by the following considerations: (a) In longitudinal impact the compressive stress is present for a longer time because of the longer distance that the wave has to travel to reach the upper edge; therefore the buckles will have more time to develop. (b) Truly square edgewise impact is unlikely to occur in practice. The package is more likely to be canted, as in Figure 5, in which case the nearly longitudinal impact (Figure 5(a)) will stress a larger area than the nearly transverse impact (Figure 5(b)).

B. Inelastic.- The formulas given above are based on the assumption that the material obeys Hooke's law, that is, that the ratio of the compressive stress σ to the corresponding strain ε is constant. In brittle materials like ceramics, the proportionality of stress to strain is thought to hold up fairly well up to the point of fracture. Therefore the assumption of Hooke's law probably does not seriously limit the validity of the Section A formulas when we are dealing with a ceramic lid or base. However, for ductile materials such as Kovar, which possess a compressive stress-strain curve like that shown in Figure 6, the linear relationship between stress and strain breaks down at a point called the "proportional limit," symbolized by P in Figure 6. Consequently, Eqs. (1), (4) and (8) are invalid for a Kovar lid or base if the stresses they predict exceed the proportional limit stress σ_p. This is possible for Eqs. (1) and (4) if the height of fall is sufficiently great and for Eq. (8) if t/a is sufficiently large. In order to allow for those possibilities we shall now generalize the considerations of Section A to the so-called inelastic case.

We shall assume that the material property information needed for this generalization is available, namely the compressive stress-strain curve, whose equation we symbolize by $\sigma = f(\varepsilon)$. From the stress-strain curve two other quantities can be obtained as functions of ε. They are the tangent modulus $E_t(\varepsilon)$ and the secant modulus $E_s(\varepsilon)$, defined by

$$E_t = df/d\varepsilon \qquad E_s = f(\varepsilon)/\varepsilon \tag{11}$$

and representing, respectively, the slope of a tangent and the slope of a secant at the point (σ,ε) (see Figure 6).

With E_t and E_s defined, we can now give the formulas related to inelastic edgewise impact, that is, impact in which v is sufficiently large to produce compressive stresses exceeding the proportional limit. When this is the case, the distribution of stress along the height of the package is no longer as shown in Figure 3. Instead the advancing stress wave has the shape shown in Figure 7, and different parts of the wave travel with different velocities, all of them less than or equal to c. The maximum compressive stress σ_{max} is of main concern to us here, along with the associated strain ε_{max}. The latter is defined implicitly by the following equation from Reference 3:

$$v = \int_0^{\varepsilon_{max}} \sqrt{E_t(\varepsilon)/\rho}\, d\varepsilon \tag{12}$$

To use this equation we need a graph of the right side as a function of its upper limit ε_{max}. Once ε_{max} is known, the corresponding stress σ_{max} can be obtained from the stress-strain curve; that is,

$$\sigma_{max} = f(\varepsilon_{max}) \tag{13}$$

Equations (13) and (12) take the place of Eq. (1) or (4) whenever the latter two lead to $\sigma > \sigma_p$.

The usual modification of Eq. (8) to account for inelastic material behavior consists of introducing a "plasticity reduction factor" η on the right side to get

$$\sigma_{cr} = \eta k E (t/a)^2 \tag{14}$$

For η we adopt the following formula from Reference 4:

$$\eta = \left(\frac{1 - \nu^2}{1 - \nu_p^2}\right)\frac{E_s}{E}\left[\frac{1}{2} + \frac{1}{2}\left(\frac{1}{4} + \frac{3}{4}\frac{E_t}{E_s}\right)^{1/2}\right] \tag{15}$$

where ν = the elastic value of Poisson's ratio ≈ 0.3 and ν_p is the plastic value given by

$$\nu_p = 0.5 - \frac{E_s}{E}(0.5 - \nu) \tag{16}$$

The E_s and E_t values in Eqs. (15) and (16) must be the ones associated with the buckling stress σ_{cr}. Therefore η is itself a function of σ_{cr}, which implies that Eq. (14) must be solved by a trial-and-error or iterative technique. However, Eq. (14) can be rewritten as

$$\sigma_{cr}/\eta = kE(t/a)^2 \tag{17}$$

and the left side plotted as a function of σ_{cr}. From this graph the value of σ_{cr} at which σ_{cr}/η equals $kE(t/a)^2$ can be picked off, thus avoiding trial-and-error or iterative calculation.

Unfortunately, the compressive stress-strain curve for Kovar does not seem to be known. We therefore omit any illustrative applications of Eqs. (11) through (17).

III. FLATWISE IMPACT

A. Elastic.- We now consider a package which impacts a rigid surface flatwise with a velocity v (Figure 8). Observations of such impact reveal that the rebound height is minute compared to the height of fall, and we shall therefore neglect rebound entirely. In that case the top of the package (we shall call it the lid for simplicity) at the instant of impact constitutes a flat plate with a uniform downward velocity

v everywhere except at the edges, where the velocity is zero. Under these initial conditions the lid will flex downward while its edges remain fixed. It will achieve some maximum central deflection (A in Figure 8), at which time its velocity will be practically zero everywhere, and then start to move upward. The problem we set for ourselves is to determine the maximum deflection A and maximum tensile stress σ'_{max} produced in the lid by any given impact velocity v.

This problem is difficult to solve exactly, but not too difficult to solve approximately if one makes some reasonable simplifying assumptions. The details of such a solution are contained in Appendix A. Those results pertinent to the constant-thickness single-material lid or base that obeys Hooke's law are embodied in Figures 9, 10 and 11.

Figure 9 and the solid curves in Figure 10 give, respectively, the *dimensionless maximum-deflection parameter* A/t and the dimensionless maximum-stress parameter $(\sigma'_{max}/E)(a/t)^2$ resulting from any given value of the dimensionless impact-velocity parameter $(v\sqrt{\rho/E})(a/t)^2$. In any particular case one can readily obtain the dimensional quantities A and σ'_{max} from the corresponding dimensionless parameters. Then, to assess their seriousness one would compare A to the internal clearance available between the lid and the package contents, and σ'_{max} to the allowable tensile stress of the lid material.*

To illustrate the use of Figures 9 and 10, let us once again consider the package of the previous examples and determine A and σ'_{max} in the ceramic base due to a flatwise drop from a height of 4 feet ($v = 16$ ft/sec) with the base up, then the same two quantities in the Kovar lid if the package were to fall with its lid up.

---

*Since σ'_{max} arises mainly from flexural action, one would be justified in comparing σ'_{max} with an allowable flexural stress or modulus of rupture.

Starting with the ceramic, we have

$$\left(\frac{a}{t}\right)^2 \frac{v}{\sqrt{E/\rho}} = \left(\frac{.92}{.03}\right)^2 \frac{16}{30,700} = .49$$

With this as abscissa and $b/a = 2.5$, Figure 9 and the solid curves of Figure 10 give

$$\frac{A}{t} = .13 \qquad \frac{\sigma'_{max}}{E}\left(\frac{a}{t}\right)^2 = 2.25$$

whence

$$A = .13(.03) = .0039 \text{ in.}$$

$$\sigma'_{max} = 2.25(47 \times 10^6)\left(\frac{.03}{.92}\right)^2 = 112,500 \text{ psi}$$

Thus, the ceramic base would experience an inward deflection of approximately four thousandths of an inch and an associated maximum tensile stress of 112,500 psi. The latter considerably exceeds the manufacturer's quoted flexural strength of 46,000 psi for the particular ceramic being considered. Thus, there is a strong likelihood of the ceramic fracturing in this impact.

Considering next the Kovar, we have

$$\left(\frac{a}{t}\right)^2 \frac{v}{\sqrt{E/\rho}} = \left(\frac{.92}{.01}\right)^2 \frac{16}{13,300} = 10.2$$

With this as abscissa and $b/a = 2.5$, Figures 9 and 10 now give

$$\frac{A}{t} = 2.7 \qquad \frac{\sigma'_{max}}{E}\left(\frac{a}{t}\right)^2 = 47$$

whence

$$A = 2.7(.01) = .027 \text{ in.}$$

$$\sigma'_{max} = 47(20 \times 10^6)\left(\frac{.01}{.92}\right)^2 = 111,000 \text{ psi}$$

Thus, we find a fairly large central deflection and maximum tensile stress. The latter is considerably above the quoted yield strength (~ 50,000 psi) of Kovar. This indicates that the more highly stressed regions of the lid will have undergone plastic deformation, and A might therefore be actually somewhat larger than the above value of .027 in., which is based on elastic theory.

The lid flexing that results from flatwise impact will induce bending moments along the edges. These are transferred to the package walls through the lid-to-wall seals, and there is a possibility of the seals being damaged by them. Figure 11 is provided to facilitate the investigation of that possibility. From Figure 11 one can determine the external hydrostatic pressure p that is equivalent to any given impact velocity v, equivalent in the sense that it will produce approximately the same elastic deformations as the impact. With p known, one can apply the formulas of Reference 5 to estimate the maximum stress S_{max} in the lid-to-wall seal.

We will illustrate the use of Figure 11 in connection with the above Kovar lid in a 16 fps flatwise impact: We enter 10.2 as the abscissa in Figure 11 and interpolate for $b/a = 2.5$ to obtain $pa^4/Et^4 = 102$. Therefore the impact is approximately equivalent to a hydrostatic pressure of

$$p = 102\ E\left(\frac{t}{a}\right)^4 = 102\ (20 \times 10^6)\left(\frac{.01}{.92}\right)^4 = 28 \text{ psi}$$

B. Inelastic.- The results presented in Section A above are based on Hooke's law. This is not a serious limitation on their applicability if we are dealing with ceramics, which, as already noted, are usually assumed to obey Hooke's law up to fracture. In the case of ductile materials, such as Kovar, however, the assumption of Hooke's law means that the results

of Section A are, strictly speaking, not valid if σ'_{max} turns out to exceed the tensile proportional limit stress. Fortunately, the exceedance is usually quite localized, which means that the computed central deflection A may still be reasonably accurate even if σ'_{max} is as high as 1.5 times the tensile yield stress σ_y (Reference 6).

For more severe impacts (which are probably beyond the range of what might be considered normal handling) the regions of plastic flow may become comparable in the extent with those of elastic deformation, and then Figure 9 might seriously under-estimate the central deflection. Unfortunately, the analysis of rectangular plates in which elastic and inelastic deformations are of comparable importance is a difficult problem, not yet solved from a practical point of view, and we shall not attempt its solution here. Paradoxically, the case of very highly developed plasticity, as might occur in extremely severe impacts, can be analyzed more easily, using the concepts of limit or yield-line analysis. This is done in Appendix B, and the main result pertinent to constant-thickness single-material lids will be described here.

This result consists of the solid lines of Figure 12. They give the maximum central deflection A of a ductile lid due to a flatwise impact so severe that the elastic deformations can be neglected in comparison with the plastic deformations. The abscissa parameter of Figure 12 involves the bending modulus of rupture σ_b of the lid, which can be easily determined through cantilever bending tests of strips of the lid material. The author has performed such tests for Kovar lids of a particular package manufacturer and arrived at the average value of $\sigma_b \approx 107$ ksi $\approx 154 \times 10^5$ psf, with a coefficient of variation of approximately 8 percent.

Figure 9 and the solid lines of Figure 12 both under-estimate A, the former because it neglects plastic deformations, the latter because they neglect elastic deformations. Therefore, for any given flatwise impact of a ductile-material lid two values of A should be computed, one from Figure 9, the other from Figure 12, and the larger of the two considered the more valid. In most cases it will be the value of A from Figure 9.

To illustrate the use of Figure 12, let us apply it to the previously considered Kovar lid in a 4-foot flatwise drop. Putting $v = 16$ ft/sec and taking the above-cited value for σ_b, we compute

$$\frac{a}{t}\frac{v}{\sqrt{\sigma_b/\rho}} = \frac{.92}{.01}\frac{16}{\sqrt{154 \times 10^5/16.2}} = 1.51$$

with this as abscissa and interpolating for $b/a = 2.5$, we find from the solid lines of Figure 12 that $A/t = .63$. This is less than the elastic value of 2.7 obtained earlier from Figure 9 for the same impact (Section IIIA). It is therefore not to be considered valid.

IV. LID WITH THINNED EDGES

When the lid has a thinned edge, as in Figure 2(b), and the thickness of the edge is much smaller than that of the rest of the lid, the bending moment capacity of the edge is very small. We shall for simplicity and conservatism neglect this capacity entirely, that is, we shall assume that the edges of the lid are "simply supported" or hinged.

This leads to the following changes in the preceding material: (a) The value of k in Eqs. (8), (14) and (17) should now be based on the dashed curve in Figure 4 (taken from Reference 7). (b) Figure 13 takes the place

of Figure 9. (c) The dashed curves of Figure 10 are to be used in place of the solid ones. And (d) the dashed lines of Figure 12 are to be used instead of the solid lines.

V. TWO-COMPONENT BASE

Here we consider a well-bonded two-component base, as in Figure 2(c), with the Young's moduli of the individual components being E_1 and E_2, the corresponding thicknesses t_1 and t_2, and the corresponding densities ρ_1 and ρ_2. Given such a base, one can determine the E, t and ρ of a single-component base that is equivalent to it in the sense that it will have the same extensional and flexural stiffnesses and the *same mass per unit area as* the two-component base. Some (but not all) of the behavior characteristics of the two-component base can then be found by applying to its one-component equivalent the formulas and charts already discussed.

The analysis to determine the E, t and ρ of the equivalent base is carried out in Appendix C with the following results:

$$t = \frac{\sqrt{4(E_1 t_1^3 + E_2 t_2^3)(E_1 t_1 + E_2 t_2) - 3(E_1 t_1^2 - E_2 t_2^2)^2}}{E_1 t_1 + E_2 t_2} \tag{18}$$

$$E = \frac{E_1 t_1 + E_2 t_2}{t} \tag{19}$$

$$\rho = \frac{\rho_1 t_1 + \rho_2 t_2}{t} \tag{20}$$

With E and ρ interpreted as above, Eq. (5) can now be used to find the compressive strain ε developed in an elastic edgewise impact of a two-component base. The corresponding stresses in the individual components will be

$$\sigma_1 = E_1\varepsilon \qquad \sigma_2 = E_2\varepsilon \tag{21}$$

in accordance with Hooke's law. The strain ε_{cr} required for elastic buckling of a two-component base can be computed from the following form of Eq. (8) with t taken from Eq. (18):

$$\varepsilon_{cr} = k(t/a)^2 \tag{22}$$

Some of the results related to flatwise impact can also be easily adapted to the two-component base by using the above interpretations of E, t and ρ. They are Figures 9 and 11.

VI. POSSIBLE SCREENING TECHNIQUES

The most realistic simulation of edgewise and flatwise impacts of a package would be obtained by actually dropping the package in a vertical or horizontal orientation, using guides to insure the maintenance of the desired orientation.

However, virtually equivalent effects can be obtained by having a massive hammer strike an initially stationary package, as in Figure 15, with a velocity equal to the impact velocity v that one wishes to simulate.

Static techniques can also be employed to produce some of the effects of edgewise and flatwise impact. For example, to simulate the compressive strain ε or ε_{max} produced by an edgewise impact (Eqs. (5) and (12)), one could place the package edgewise between the heads of a universal testing machine and let the heads come together an appropriate amount. (This assumes the package walls are flat and parallel so that

proper contact can be maintained with the testing machine heads.) To simulate a flatwise impact, one could subject the package to external hydrostatic pressure in a pressure vessel, choosing the pressure on the basis of Figure 11 or 14.

By such techniques it should be possible to assess the vulnerability of a package type to damage in what we might call a "standardized" normal handling, as represented by purely edgewise or flatwise impact in a fall.

Of course, the falls that might occur in actual normal handling are unlikely to be purely edgewise or flatwise. Therefore a supplementary screen would be desirable, involving falls with <u>random</u> orientations. This supplementary screen could be dispensed with if experiments (proposed in Section VII) indicated that the purely edgewise and flatwise impacts were a sufficiently valid representation of random-orientation impacts.

VII. SUGGESTIONS FOR FURTHER RESEARCH

The studies in Sections II and III clearly predict that normal handling, as represented by the fall of a package onto a floor, can be a significantly stressful and damaging condition for an electronic package. It is therefore important to test the accuracy and validity of those studies by means of experiments. If these experiments confirm the accuracy and validity of the studies, then it becomes important to devise adequate screens to detect those packages that are most vulnerable to damage in such normal handling. A program to accomplish these objectives is described below.

A. Experiments to Test Accuracy of the Theory.- By instrumenting a package with strain gages, it should be possible to measure the compressive strain ε produced in the lid or base during a carefully controlled edgewise impact, and thus check the accuracy of Eq. (5).

Similarly, by measuring the flexural strains of a lid or base in a carefully controlled flatwise impact, and converting those measurements to a deflection A, one can check the accuracy of Figures 9 and 13.

The postulated equivalence of external pressure and flatwise impact (Figures 11 and 14) can be checked by exposing the instrumented package to external pressure in a pressure vessel, measuring the central flexural strains in the lid and base, and comparing those strains with the ones measured in the supposedly equivalent flatwise impacts.

B. Experiments to Test Validity of the Theory.- The theoretical studies of Sections II and III assumed rather idealized impacts -- purely edgewise and purely flatwise. In an actual fall the orientation of the package at impact cannot be controlled. Therefore, the question naturally arises as to whether the idealized impacts are a valid representation of actual (i.e., random-orientation) impacts, valid in the sense that they produce stresses of comparable magnitude to those produced by the actual impacts, or, if not of comparable magnitude, stresses that have some consistent correlation with those produced by the actual impacts.

This question can best be answered by experiments in which instrumented packages are subjected to both random-orientation impacts and carefully controlled impacts. By comparing the strains obtained in the two types of impact, one can judge the extent to which the latter are a valid representation of the former.

C. Development of Screening Procedures.- Assuming that the experiments proposed above will confirm the predicted seriousness of the fall of a package from a small height, it then becomes important to devise a simple, practical and valid screening procedure that will cull from a group of packages those most vulnerable to damage in such a fall.

As discussed in Section VI, there are several options for the nature of the screen. In order of increasing realism, they are:

(a) static tests involving edgewise compression in a testing machine and external hydrostatic pressure in a pressure vessel;

(b) hammer blows producing idealized impacts (purely edgewise and flatwise) on an initially stationary package;

(c) controlled-orientation drop tests producing idealized impacts (purely edgewise and flatwise); and

(d) random-orientation drop tests.

The decision as to which of those options is best must await the outcome of the tests discussed in Section B above. Option (d) is the most realistic and appears to be simple, but may require a larger number of tests than the other options to be statistically significant. Therefore one of the other options may be preferable, provided that it is shown to be a sufficiently valid representation of option (d).

D. Tests to Obtain Compression Data for Kovar.- It was pointed out in Section IIB that when the compressive stress σ_{max} produced in a Kovar lid by edgewise impact exceeds the proportional limit stress σ_p, the prediction of σ_{max} requires a knowledge of the compressive stress-strain curve $\sigma = f(\varepsilon)$. This curve is also needed to predict the buckling stress σ_{cr} when that stress exceeds σ_p.

Unfortunately, the compressive stress-strain curve for Kovar does not seem to be available in the literature, nor from the various DoD information centers, nor from its manufacturers. Therefore, edgewise

compression tests of suitably supported Kovar sheets typical of those used for package lids should be conducted in order to obtain this necessary item of information.

VIII. CONCLUDING REMARKS

In this report theoretical studies have been made of the stresses and deflections produced in flat-pack lids and bases by "normal handling," where this is interpreted to be the fall of the package from a small height leading to purely edgewise or purely flatwise impact.

The studies have shown that the stresses due to such normal handling can be severe, sufficiently so as to buckle a metallic lid or crack a ceramic lid or base.

The severity of these stresses suggests that a screening procedure would be desirable whereby packages most vulnerable to damage in this kind of normal handling can be weeded out, and several options for the nature of such a screen have been discussed.

Finally, further work of an experimental nature has been suggested for the purpose of: (a) testing the accuracy of the theoretical analyses in the present report, (b) determining if the idealized impacts (edgewise and flatwise) assumed in these analyses can be considered equivalent to more realistic (random-orientation) impacts, (c) arriving at a simple, practical and valid screening procedure, and (d) obtaining needed compression stress-strain data for Kovar.

Further work of a theoretical nature would also be desirable in order to assess the effects of impact on the internal components of a package, such as wires, wire bonds, dies and substrates.

APPENDIX A: ANALYSIS OF FLATWISE ELASTIC IMPACT

We outline here the analyses leading to Figures 9, 10, 11, 13 and 14. We start with those analyses that pertain to the constant-thickness lid or base, which can be considered clamped along its edges by virtue of its attachment to generally short stubby walls. The coordinate system to be employed is shown in Figure 16.

As discussed in Section IIIA, we shall consider the upper surface of the package in flatwise impact to be a plate moving with a uniform downward velocity v and having its boundary instantaneously arrested. We shall also assume that for any central deflection A the state of deformation in the plate is the same whether that deflection is produced by a statically applied uniform lateral pressure or by the dynamic flexing of the plate resulting from the arrest of its edges. Furthermore, we shall assume that in either of these two conditions the normal deflection $w(x,y)$ can be represented with sufficient accuracy by the single-degree-of-freedom function

$$w = Af(x,y) \tag{A1}$$

where A is central deflection and $f(x,y)$ is the following approximation to the deflection surface of a clamped plate with unit central deflection and $b \geq a$:

$$f(x,y) = \begin{cases} \frac{1}{4}\left(1 - \cos\frac{2\pi x}{a}\right)\left(1 - \cos\frac{2\pi y}{a}\right) & \text{in Region 1} \\ \frac{1}{2}\left(1 - \cos\frac{2\pi y}{a}\right) & \text{in Region 2} \\ \frac{1}{4}\left(1 - \cos\frac{2\pi (b-x)}{a}\right)\left(1 - \cos\frac{2\pi y}{a}\right) & \text{in Region 3} \end{cases} \tag{A2}$$

The regions referred to in Eq. (A2) are defined in Figure 16.

From Eqs. (A1) and (A2) we obtain the following "deflection volume" V associated with any central deflection A, that is, the volume between the deflected and undeflected configurations of the plate middle surface:

$$V = \int_0^a \int_0^b w(x,y)dx\,dy = \frac{Aa^2}{4}\left(2\frac{b}{a} - 1\right) \qquad (A3)$$

If the central deflection A were produced by a static uniform pressure p, one could obtain the relationship between p and A from available elastic solutions. One such solution, which accounts for membrane as well as flexural action and assumes that the edges are unrestrained against in-plane movement, is given in Reference 5 in the form

$$\frac{A}{t} = C\frac{pa^4}{Et^4}n_4n_5 \qquad (A4)$$

where C is a not very sensitive function of Poisson's ratio (we shall use C = 11.2, which corresponds to a Poisson's ratio of 0.25); n_5 is a function of b/a and pa^4/Et^4 which accounts for membrane action and which is plotted against pa^4/Et^4 in Figure 12(c) of Reference 5; and n_4 is the following function of b/a obtained from Table 35 of Reference 8 or Figure 11 of Reference 5 with K = ∞:

b/a	1.0	1.25	1.5	2.0	3.0	∞
n_4	.00126	.00182	.00220	.00254	.00259	.00260

(A5)

Finally, the plate strain energy SE associated with any pressure or central deflection can be obtained by computing the work done by the pressure in producing the deflection volume V. That is,

$$SE = \int_o^V pdV \tag{A6}$$

From (A3)

$$dV = \frac{a^2}{4}\left(2\frac{b}{a} - 1\right)dA \tag{A7}$$

and from (A4)

$$dA = Ctn_4\, d\left(\frac{pa^4}{Et^4} n_5\right) \tag{A8}$$

We can substitute (A8) into (A7), then (A7) into (A6), and use the notation

$$y \equiv pa^4/Et^4 \tag{A9}$$

$$n_5 = g(y) \tag{A10}$$

to obtain

$$SE = \frac{CEt^5 n_4}{a^2}\left(\frac{b}{2a} - \frac{1}{4}\right)\int_o^{yg(y)} y'd[y'g(y')] \tag{A11}$$

where y' is a dummy variable representing y. With the integral on the right side evaluated numerically, Eq. (A11) gives the strain energy as a function of pa^4/Et^4. Since pa^4/Et^4 is related to A through Eq. (A4), the strain energy is also implicitly known as a function of the central deflection A.

With the aid of the above results, we can now determine what static pressure p will produce the same central deflection A as a given impact velocity v. To do this, we assume a conservative system

and equate the kinetic energy at zero deflection ($\rho abtv^2/2$) to the strain energy (A11) at maximum deflection. This leads to the following implicit equivalence relationship between static pressure p and flatwise impact velocity

$$\left(\frac{a}{t}\right)^2 \frac{v}{\sqrt{E/\rho}} = \sqrt{Cn_4\left(1 - \frac{1}{2}\frac{a}{b}\right)h(y)} \qquad \text{(A12)}$$

where $h(y) = h(pa^4/Et^4)$ stands for the integral on the right side of Eq. (A11), regarded as a function of y, i.e., of pa^4/Et^4. Elimination of pa^4/Et^4 between Eqs. (A12) and (A4) then leads to the curves of Figure 9. To obtain the solid curves of Figure 10, use is made of the following relationship from Reference 5:

$$\sigma'_{max} = n_7 E \cdot (t/a)^2 \qquad \text{(A13)}$$

where n_7 is the function of b/a and pa^4/Et^4 plotted against the latter parameter in Figure 14(c) of Reference 5. Elimination of pa^4/Et^4 between Eqs. (A13) and (A12) leads to the solid curves of Figure 10.

For A/t sufficiently small (say less than unity), membrane action is negligible, which implies that $n_5 = g(y) = 1$. This simplifies Eqs. (A4) and (A12) to

$$\frac{A}{t} = C \frac{pa^4}{Et^4} n_5 \qquad \text{(A14)}$$

$$\left(\frac{a}{t}\right)^2 \frac{v}{\sqrt{E/\rho}} = \frac{pa^4}{Et^4}\sqrt{\frac{1}{2} Cn_4\left(1 - \frac{1}{2}\frac{a}{b}\right)} \qquad \text{(A15)}$$

Elimination of pa^4/Et^4 between these two equations gives

$$\frac{A}{t} = \sqrt{\frac{2Cn_4}{1 - \frac{1}{2}\frac{a}{b}}} \left(\frac{a}{t}\right)^2 \frac{v}{\sqrt{E/\rho}} \qquad \text{(A16)}$$

Equations (A15) and (A16) represent the linear portions of the solid curves in Figures 11 and 9, respectively.

The analysis related to a lid with thinned edges which are idealized as hinged or simply supported proceeds along similar lines, starting with the following assumed $f(x,y)$ in place of Eq. (A2):

$$f(x,y) = \begin{cases} \sin\frac{\pi x}{a} \sin\frac{\pi y}{a} & \text{in Region 1} \\ \sin\frac{\pi y}{a} & \text{in Region 2} \\ \sin\frac{\pi(b-x)}{a} \sin\frac{\pi y}{a} & \text{in Region 3} \end{cases} \qquad \text{(A17)}$$

This leads to the following V formula in place of Eq. (A3):

$$V = Aa^2 \left(\frac{2}{\pi}\frac{b}{a} - \frac{2}{\pi} + \frac{4}{\pi^2}\right) \qquad \text{(A18)}$$

The deflection-pressure relationship is still of the form (A4), but n_5 is now given by Figure 12(a) of Reference 5, and n_4 is now the following function of b/a (from Table 8 of Reference 8 or Figure 11 of Reference 5 with $K = 0$):

b/a	1	1.25	1.5	2	3	∞
n_4	.00406	.00600	.00772	.01013	.01223	.01302

The strain energy formula replacing (A11) is

$$SE = \frac{\alpha C E t^5 n_4}{a^2} \int_0^{yg(y)} y' d[y'g(y')] \qquad (A20)$$

where α is the term in parentheses in Eq. (A18).

The pressure-velocity equivalence then becomes

$$\left(\frac{a}{t}\right)^2 \frac{v}{\sqrt{E/\rho}} = \sqrt{2 \frac{a}{b} \alpha C n_4 \, h(y)} \qquad (A21)$$

in place of (A12), and this equation leads to the curves of Figure 14. Elimination of pressure between Eqs. (A21) and (A4) then gives the deflection-velocity relationship of Figure 13. The stress versus pressure relationship may still be expressed as Eq. (A13) but with n_7 now taken from Figure 14(a) of Reference 5. Elimination of pressure between Eqs. (A21) and (A13) will then lead to the dashed curves of Figure 10.

The small-deflection linearization is effected as before by setting $n_5 = g(y) = 1$, and it gives in this case

$$\left(\frac{a}{t}\right)^2 \frac{v}{\sqrt{E/\rho}} = \frac{p a^4}{E t^4} \sqrt{\frac{a}{b} \alpha C n_4} \qquad (A22)$$

$$\frac{A}{t} = \sqrt{\frac{b}{a} \frac{C n_4}{\alpha}} \left(\frac{a}{t}\right)^2 \frac{v}{\sqrt{E/\rho}} \qquad (A23)$$

These equations represent the straight-line portions of Figures 14 and 13, respectively.

APPENDIX B: ANALYSIS OF FLATWISE INELASTIC IMPACT

A "rigid-plastic" analysis will here be used to determine the central deflection A of a clamped rectangular plate resulting from an extremely large flatwise impact velocity v in which there is no rebound of the plate edges. In this analysis elastic deformations are neglected and the entire deformation is assumed to consist of a pattern of folds along plastic hinges which are represented by the dashed lines in Figure 17. Simple geometrical considerations give the angle of fold θ along each hinge line as a function of A, and these relationships are given in Figure 17.

The energy dissipated along any hinge line is computed as the product θmL, where θ is the angle of fold for that hinge line, L is its length, and m is the "fully plastic bending moment" per unit width for the material. The fully plastic bending moment m is related as follows to the flexural strength or bending modulus σ_b and the thickness t of the plate:

$$m = \sigma_b t^2/6 \tag{B1}$$

Forming the product θmL for each of the nine hinge lines shown in Figure 17 and summing, we obtain the following energy dissipation associated with the assumed hinge-line pattern:

$$\text{Dissipated energy} = 4mA \left(2\frac{b}{a} + \frac{a}{\beta b}\right) \tag{B2}$$

Up to this point the value of β has been left unspecified. We shall now assume that β has the same value as in a yield-line analysis under uniform lateral pressure. This can be shown to be

$$\beta = -\frac{1}{2}\left(\frac{a}{b}\right)^2 + \frac{1}{2}\sqrt{\left(\frac{a}{b}\right)^4 + 3\left(\frac{a}{b}\right)^2} \tag{B3}$$

The central deflection A produced by an impact velocity v can now be obtained by equating the initial kinetic energy ($\rho abtv^2/2$) to the energy (B2) dissipated in plastic bending along the hinge lines. With m and β replaced by their expressions (B1) and (B3), this equality leads to the following deflection-velocity relatively.

$$\frac{A}{t} = \frac{3(b/a)}{4Z} \left(\frac{a}{t} \frac{v}{\sqrt{\sigma_b/\rho}}\right)^2 \tag{B4}$$

where

$$Z \equiv \frac{2}{3}\left[\frac{a}{b} + 3\frac{b}{a} + \sqrt{\left(\frac{a}{b}\right)^2 + 3}\right] \tag{B5}$$

Equation (B4) is plotted as the solid lines in Figure 12.

If the plate is simply supported, the outer yield lines of Figure 17 are non-existent. The energy dissipation will then turn out to be just half of that given by Eq. (B2), and the deflection will be twice that given by Eq. (B4). The dashed lines in Figure 17 give the deflection-velocity relationship in that case.

APPENDIX C: SINGLE-COMPONENT EQUIVALENT OF A TWO-COMPONENT BASE

Figure 18(a) shows a one-component and a two-component bar, both of unit length and unit width (perpendicular to the paper). It is assumed in each case that Hooke's law holds and that plane cross sections remain plane and perpendicular to the axis of the bar. For the two component bar, we shall also assume that both components have the same Poisson's ratio.

Figure 18(b) shows both bars subjected to an imposed pure elongation e and gives the tension force P needed to produce this elongation. In order for the stretching stiffness P/e to be the same

for both bars, it is seen that the following relation must hold among the elastic constants:

$$Et = E_1 t_1 + E_2 t_2 \tag{C1}$$

Figure 18(c) shows both bars this time subjected to pure bending moments of magnitude M. Elementary beam theory gives the relationships shown in the figure between M and the resulting curvatures θ. In order for both bars to have the same bending stiffness M/θ, it is clearly necessary that

$$\frac{Et^3}{12} = \frac{4(E_1 t_1^3 + E_2 t_2^3)(E_1 t_1 + E_2 t_2) - 3(E_1 t_1^2 - E_2 t_2^2)^2}{12(E_1 t_1 + E_2 t_2)} \tag{C2}$$

If Eqs. (C1) and (C2) are solved simultaneously for t and E, Eqs. (18) and (19) result. These are the t and E of a single-component plate that is elastically equivalent to the two-component plate.

For dynamical equivalence, we require that the mass per unit area should also be the same in the two plates; that is,

$$\rho t = \rho_1 t_1 + \rho_2 t_2 \tag{C3}$$

and this leads to Eq. (20) for the required density ρ of the single-component plate.

REFERENCES

1. S. P. Timoshenko and J. N. Goodier: Theory of Elasticity, 3rd edition, McGraw-Hill Book Co., New York, 1970, Chapter 14.

2. C. Libove and M. Stein: Charts for Critical Combinations of Longitudinal and Transverse Direct Stress for Flat Rectangular Plates, NACA ARR L6A05, March 1946. (Reissued as NACA Wartime Report L-224.)

3. W. Johnson: Impact Strength of Materials, Crane, Russak, New York, 1972, p. 216.

4. G. Gerard: Introduction to Structural Stability Theory, McGraw-Hill Book Co., Inc., New York, 1962, pp. 52, 58 and 160.

5. C. Libove: Rectangular Flat-Pack Lids Under External Pressure: Improved Formulas for Screening and Design, RADC-TR-76-291, September 1976, AD# A032490.

6. B. Aalami and D. G. Williams: Thin Plate Design for Transverse Loading, John Wiley and Sons, New York, 1975, p. 36.

7. S. P. Timoshenko and J. M. Gere: Theory of Elastic Stability, 2nd edition, McGraw-Hill Book Co., Inc., New York, 1961, Section 9.2.

8. S. P. Timoshenko and S. Woinowsky-Krieger: Theory of Plates and Shells, 2nd edition, McGraw-Hill Book Co., Inc., New York, 1959.

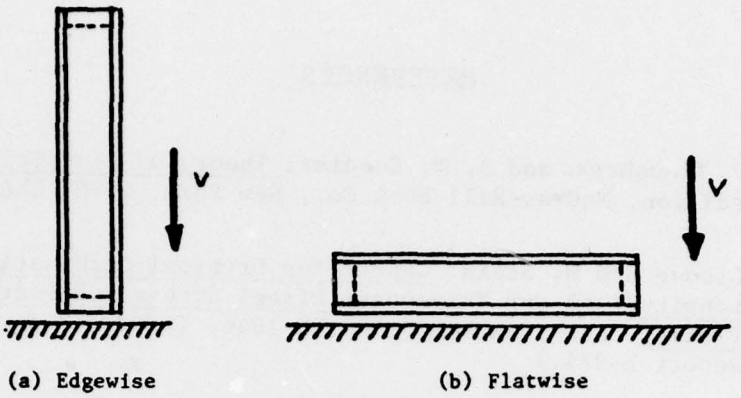

Figure 1.- Two idealized modes of impact of a rectangular flat-pack on a rigid floor. (v = velocity of impact.)

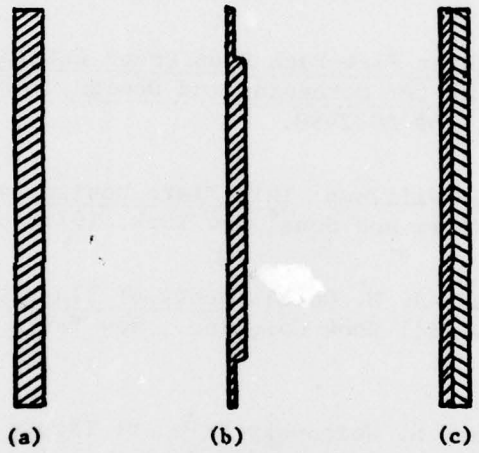

Figure 2.- Lid and base variations considered: (a) Constant-thickness lid or base. (b) Lid with thinned edges. (c) Two-component base.

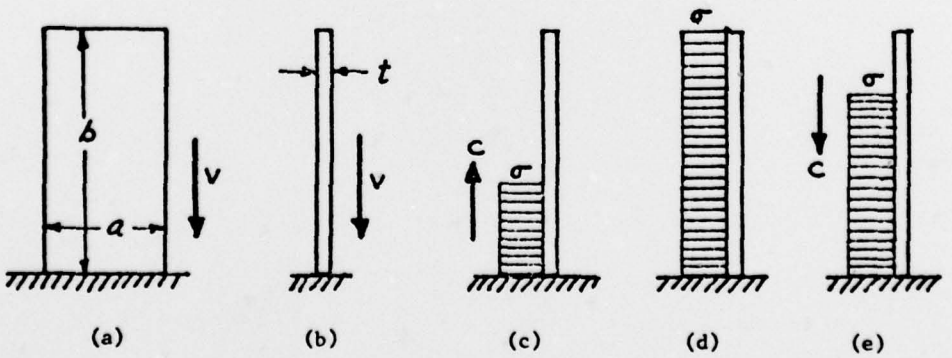

Figure 3.- Edgewise impact of lid or base on rigid surface. (a) Front view. (b) Side view. (c) Compressive stress wave travelling upward. (d) Wave front has reached top edge. (e) Unloading wave travelling downward. (v = impact velocity; c = speed of sound in the material.)

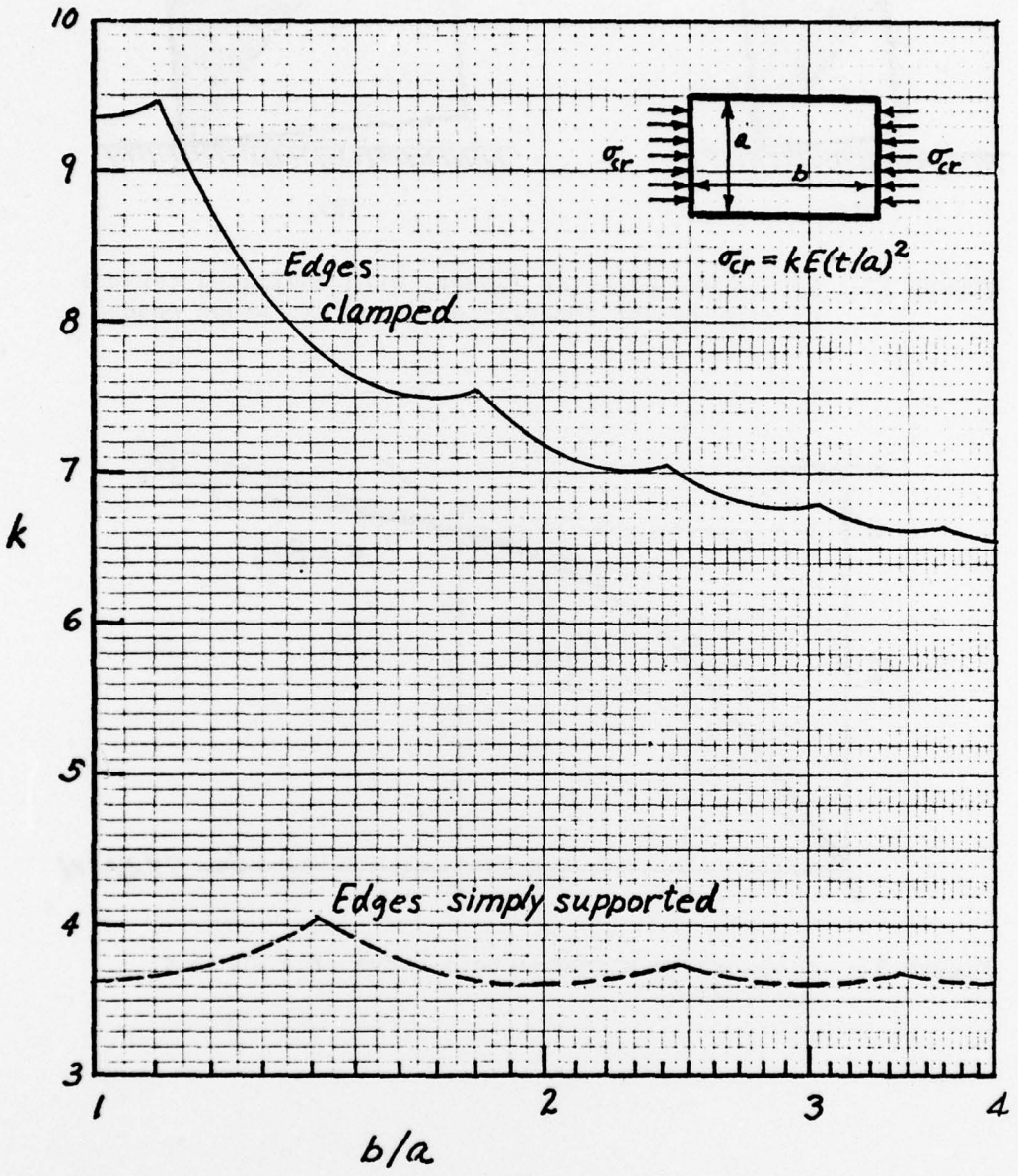

Figure 4.- Buckling stress coefficient for rectangular elastic plates in longitudinal compression (Poisson's ratio taken as 0.3).

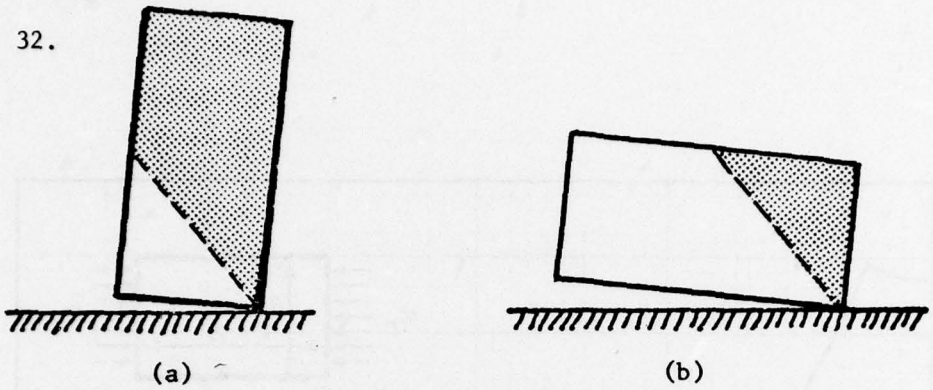

Figure 5.- Non-square edgewise impact, with estimated regions of significant impact-induced stress shown shaded.

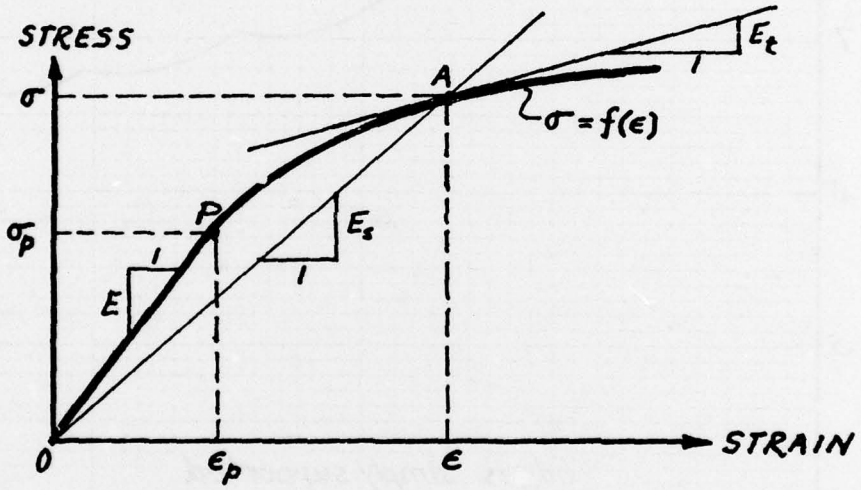

Figure 6.- Compressive stress-strain curve of a ductile material.

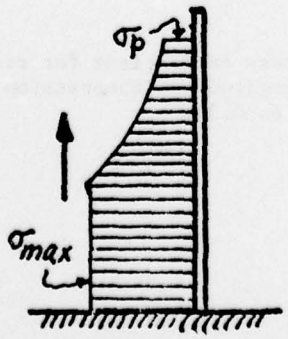

Figure 7.- Shape of advancing stress wave in inelastic impact.

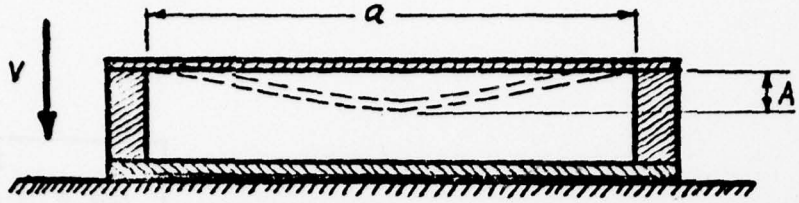

Figure 8.- Flatwise impact of a package on a rigid surface.

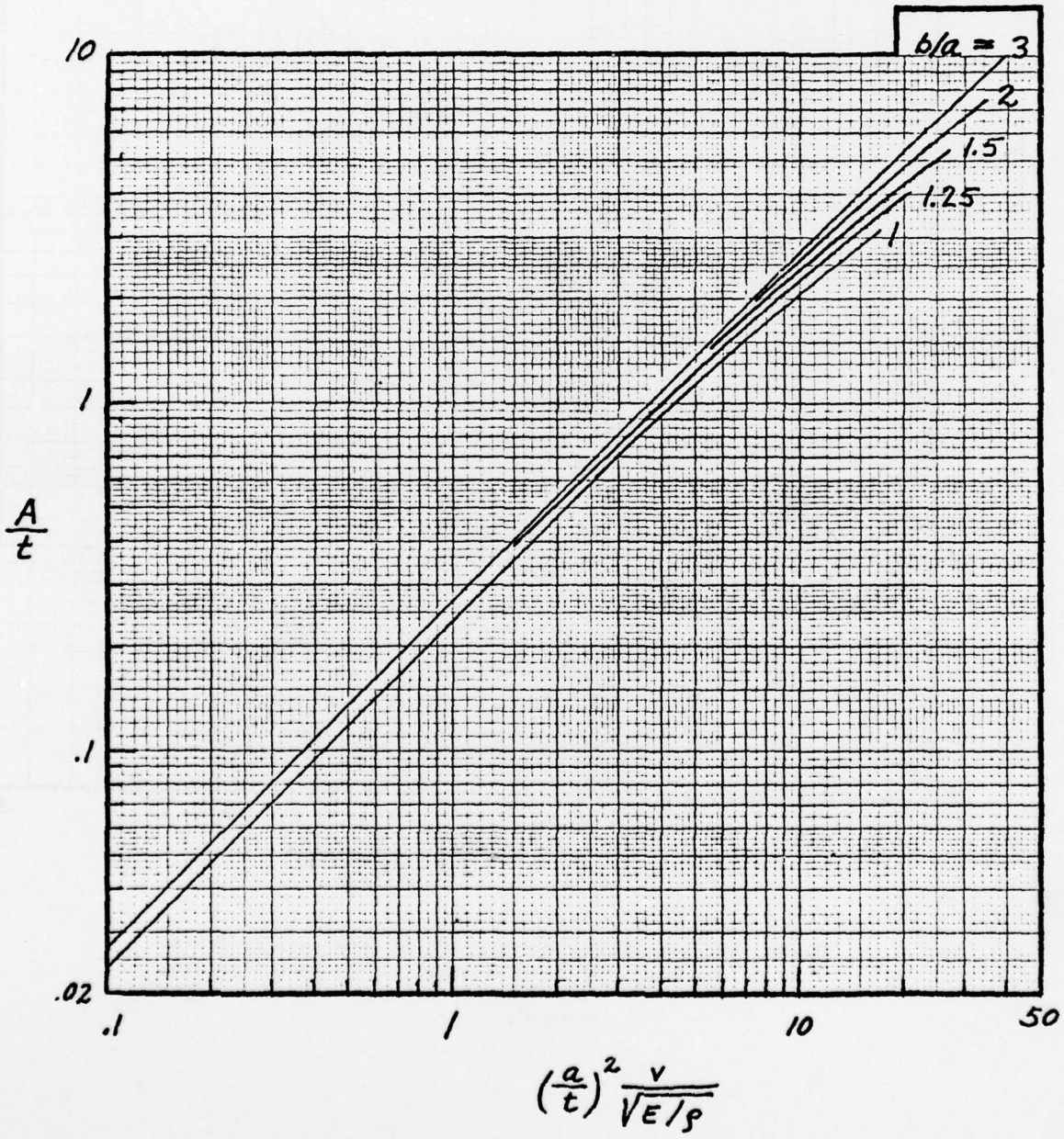

Figure 9.- Graphs for determining maximum central deflection A of a clamped rectangular lid or base resulting from flatwise impact. (Based on elastic theory.)

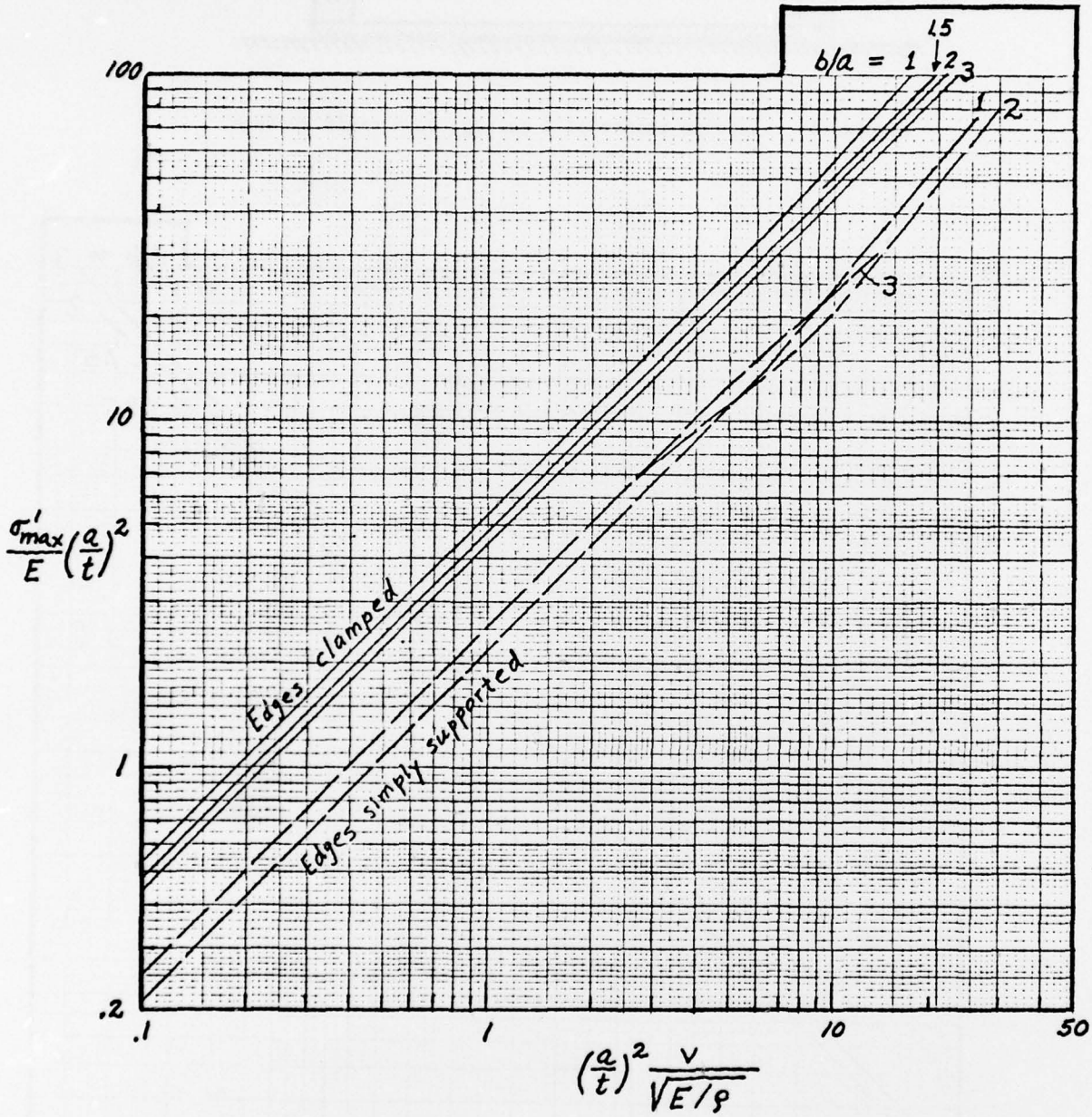

Figure 10.- Graphs for determining maximum tensile stress σ'_{max} in a rectangular lid or base resulting from flatwise impact. (Based on elastic theory.)

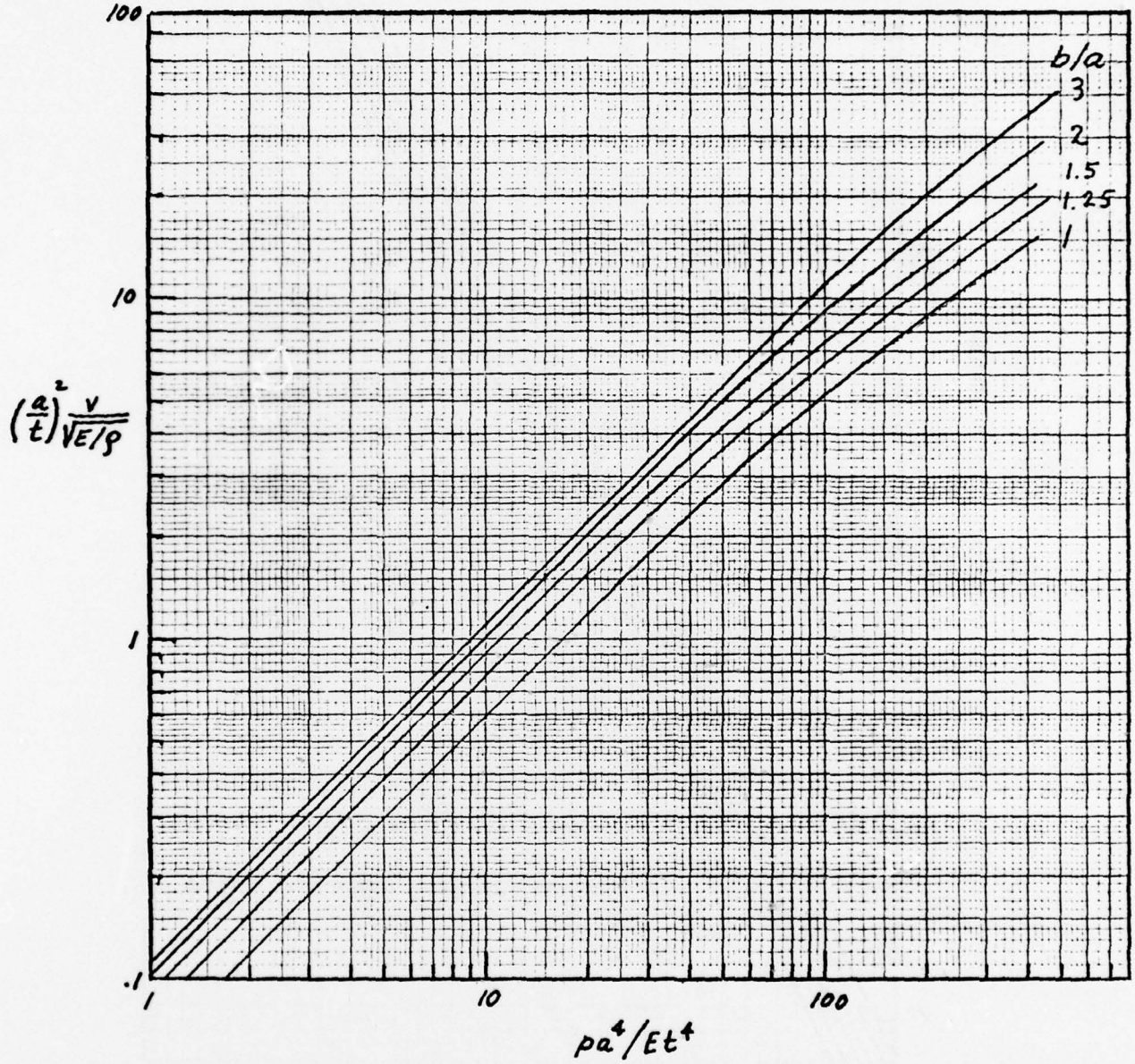

Figure 11.- Graphs for determining hydrostatic pressure p equivalent to a given impact velocity v for a clamped rectangular lid or base. (Based on elastic theory.)

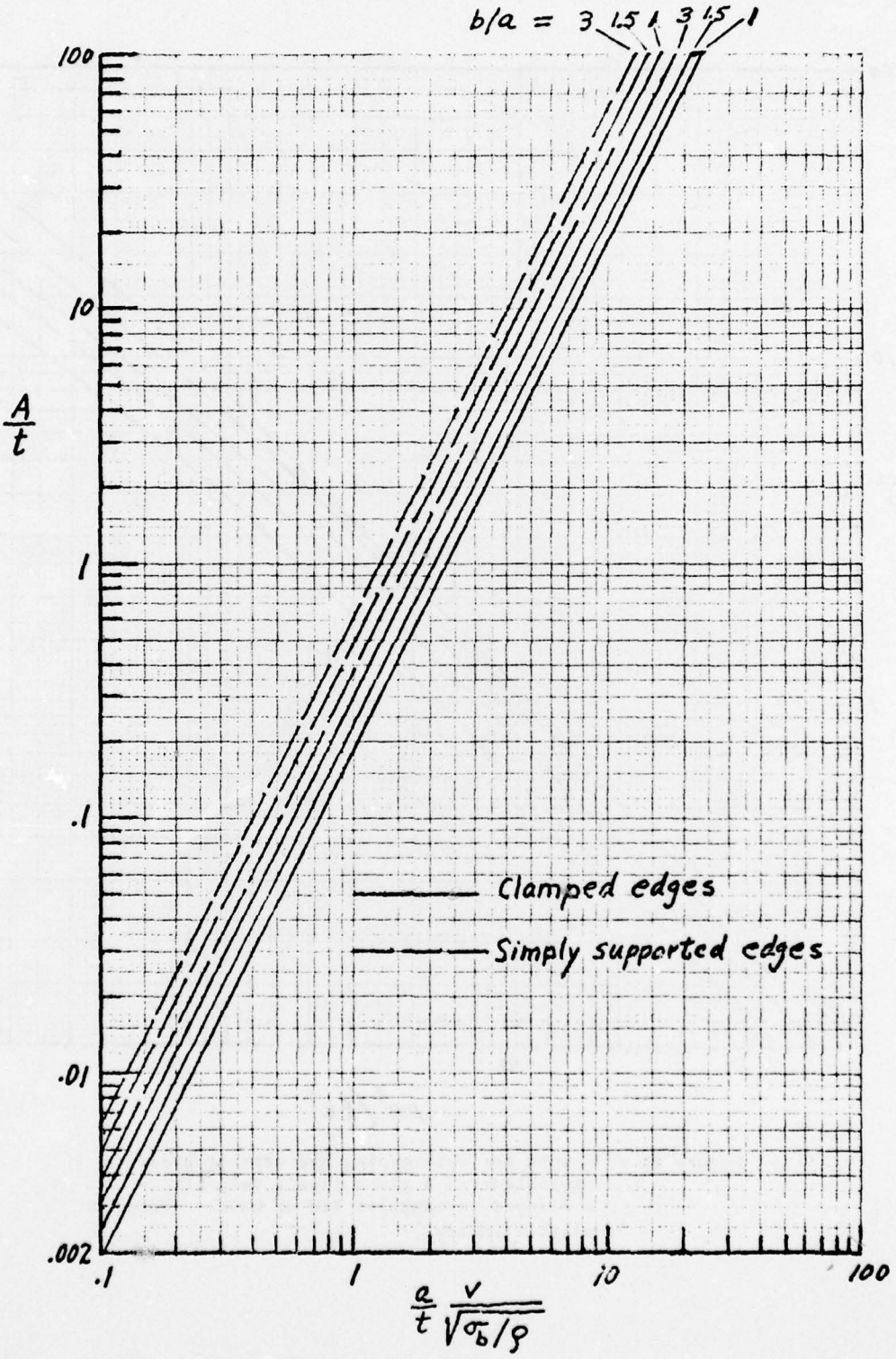

Figure 12.- Graphs for determining maximum central deflection A of rectangular ductile lid resulting from severe flatwise impact. (Based on yield-line analysis.)

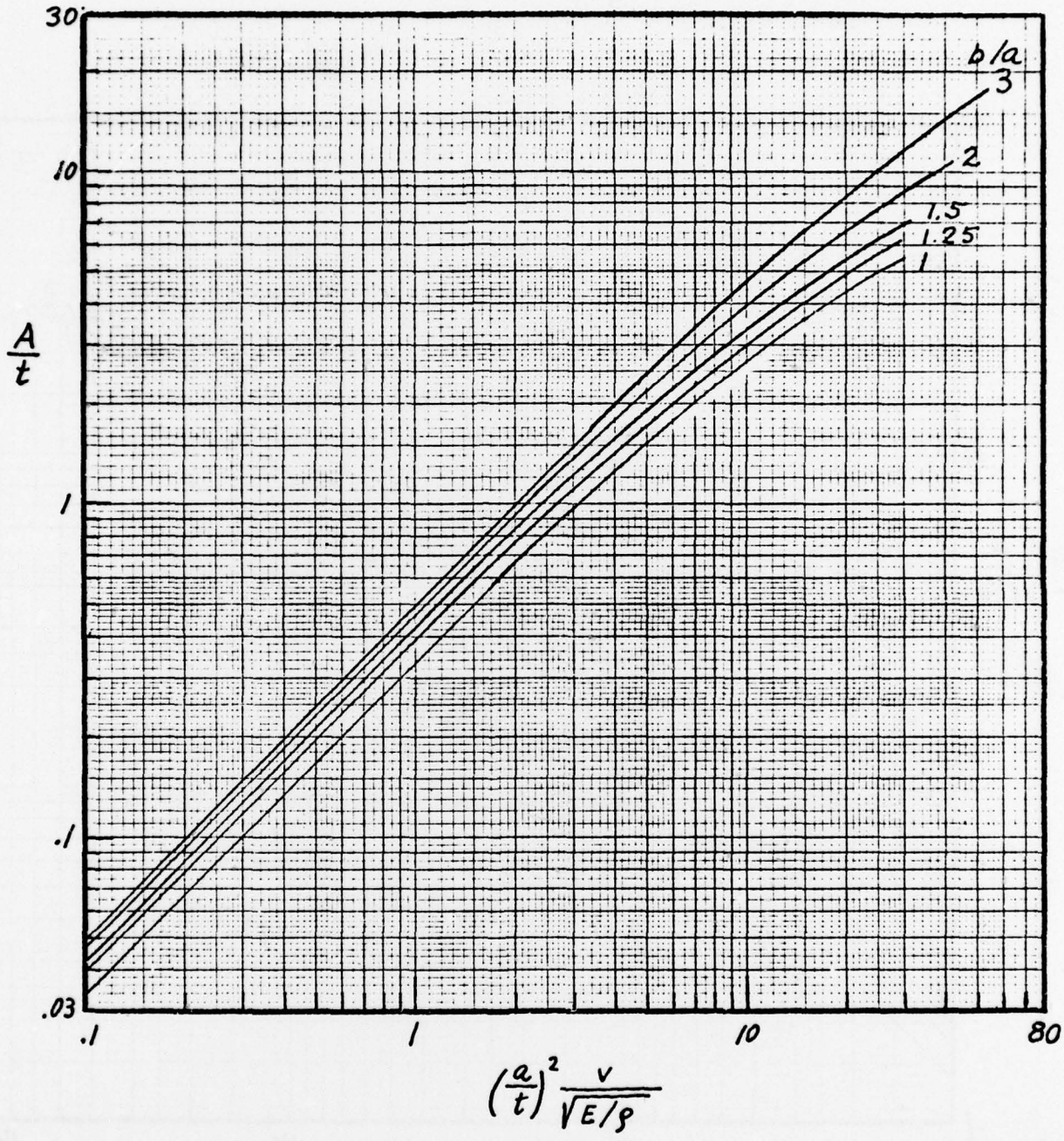

Figure 13.- Graphs for determining maximum central deflection A of a simply supported rectangular lid resulting from flatwise impact. (Based on elastic theory.)

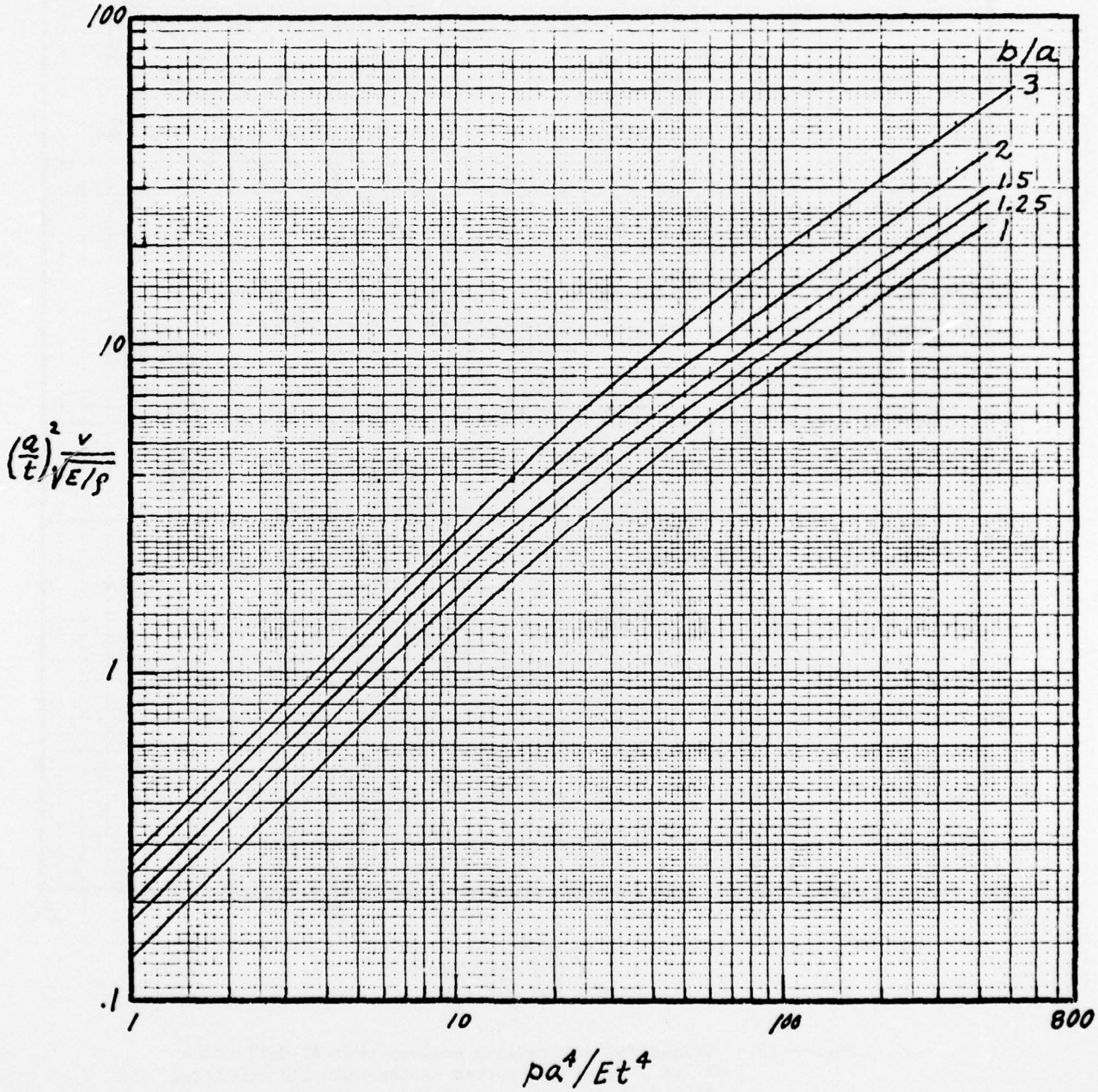

Figure 14.- Graphs for determining hydrostatic pressure p equivalent to a given flatwise impact velocity v for a simply supported rectangular lid. (Based on elastic theory.)

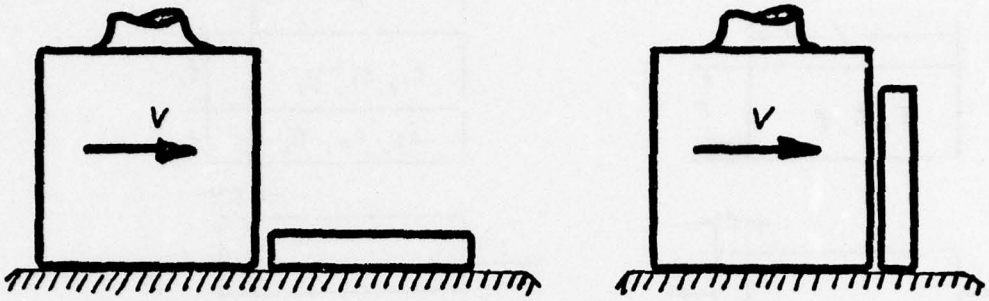

(a) Edgewise (b) Flatwise

Figure 15.- Simulation of floor drop impacts through a hammer blow.

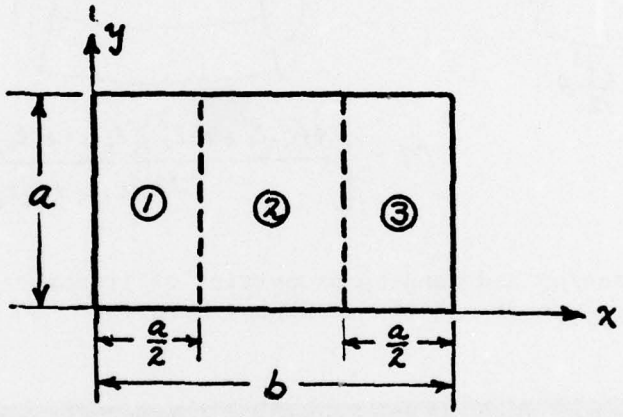

Figure 16.- Coordinate System.

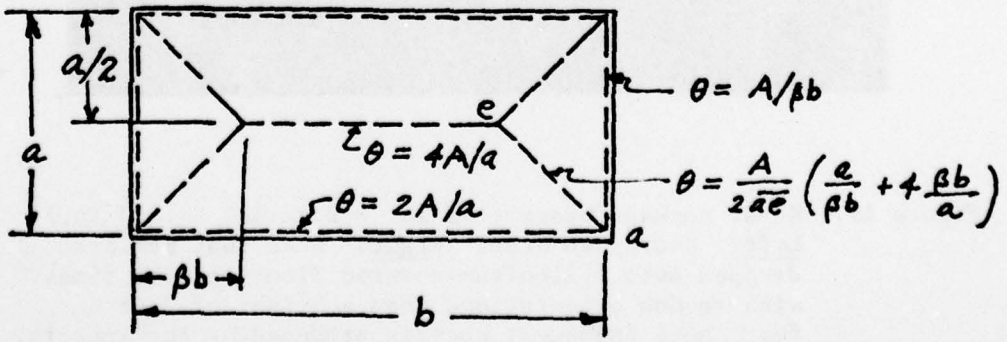

Figure 17.- Yield-line pattern assumed for extreme inelastic flatwise impact of clamped rectangular plate.

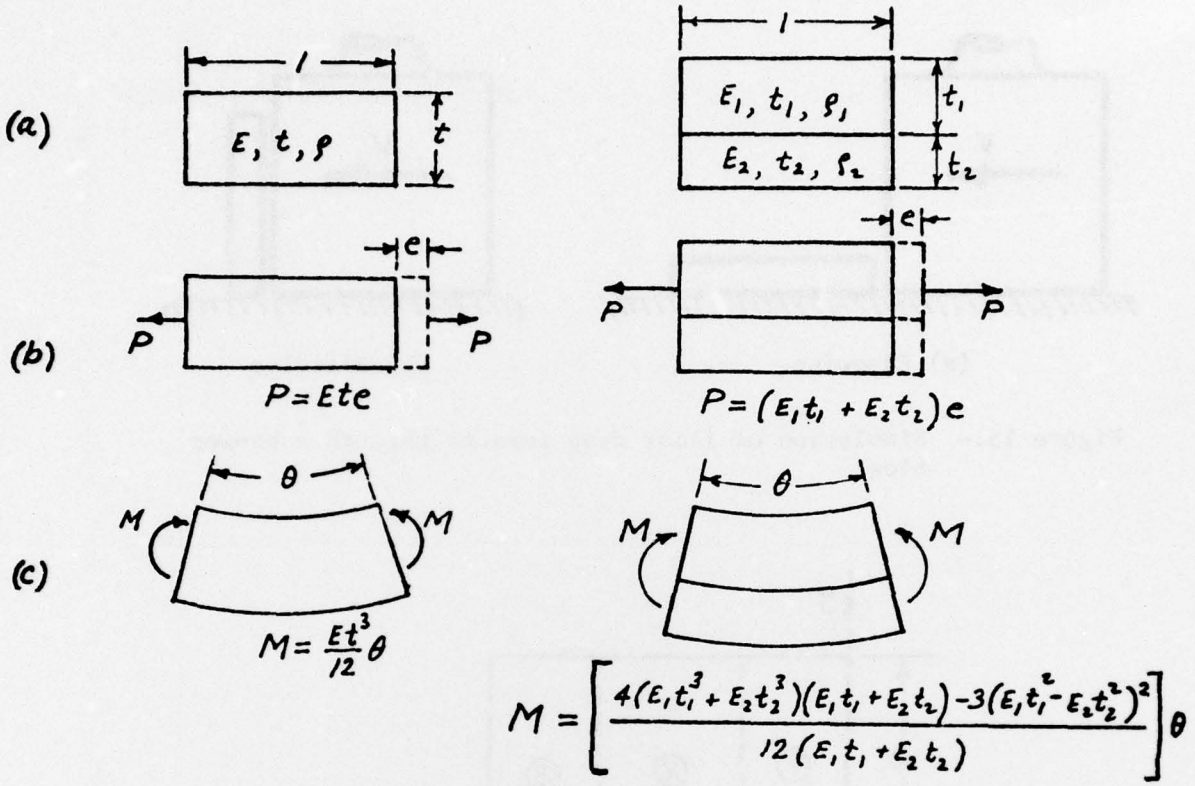

Figure 18.- Stretching and bending properties of linearly elastic one-component and two-component bars.

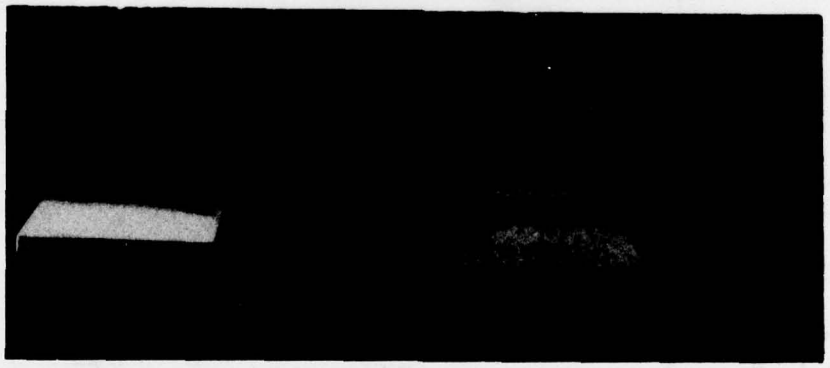

Figure 19.- Kovar package bases (.92 in. × 2.22 in. × .010 in.) Left: Undropped base. Right: Base that had been dropped onto a linoleum-covered floor several times with random orientations from a height of 3 or 4 feet; note permanent buckles produced by the impacts.